JREE: Vol. 12, No. 4, (Autumn 2025) 9-20

Journal of Renewable Energy and Environment

Journal Homepage: www.jree.ir

Materials and Energy Research Center

MERC

Research Article

Development and Performance Analysis of a Composite Hydrodynamic Cavitation Reactor for Biodiesel Production

Yosuf Nosrati[a], Hossein Javadikia[a*], Leila Naderloo[a*], Mostafa Mostafaei[a,b]

[a] *Department of Mechanical Biosystems Engineering, Faculty of Agriculture, College of Agriculture and Natural Science, Razi University, Kermanshah, Iran.*
[b] *Biosystems Engineering Department, Faculty of Agriculture, University of Tabriz, Tabriz, Iran.*

PAPER INFO

Paper history:
Received: 27 October 2024
Revised: 30 May 2025
Accepted: 07 September 2025

Keywords:
Biodiesel Fuel,
Compound Reactor,
Hydrodynamic Cavitation,
Intensity of Reaction,
Process Intensification,
Sustainable Energy,
Trans-Esterification Reaction

ABSTRACT

Biodiesel can be produced through various methods, but the transesterification reaction is the most widely used due to its advantages, such as improved biodiesel quality, continuous in-line processing, reduced methanol and catalyst requirements, and enhanced energy efficiency. Recent advancements in biodiesel production technology have focused on optimizing the mixing process and improving mass and heat transfer between the two liquid phases involved in the transesterification reaction. These innovations have led to the development of new reactors that significantly increase reaction rates and reduce production time. In this study, the design and construction of a novel hydrodynamic cavitation reactor—a commercially viable renewable energy system—were investigated. After its construction and commissioning, the reactor was tested using standard biodiesel production materials. The evaluation results demonstrated that the optimal reaction time for biodiesel production was 3.13 minutes, with a rotational speed of 16,000 rpm and a flow rate of 0.83 liters per minute. The biodiesel produced met high-quality standards and complied with international fuel specifications. The highest hydrodynamic cavitation efficiency achieved was 6.19 mg/kJ. The results indicated that the transesterification reaction efficiency exceeded 88% at 3.13 minutes using this hydrodynamic cavitation reactor, highlighting an excellent recovery time for crude biodiesel production. This method significantly reduces processing time compared to conventional biodiesel production reactors, which typically require more than 20 minutes to over an hour to complete the process. The successful design, commissioning, and biodiesel production using this reactor represent a significant step forward in intensifying and optimizing the biodiesel production process.

https://doi.org/10.30501/jree.2025.482479.2115

1. INTRODUCTION

Due to environmental pollution caused by fossil fuel emissions and their non-renewable nature, the use of clean fuels such as biodiesel has become increasingly important. According to fuel standards, biodiesel is composed of high alkyl esters of fatty acid chains derived from the reaction of an alcohol with a renewable lipid source (Monika, Banga, & Pathak, 2023). In addition to fresh straight vegetable oil (SVO), biodiesel can also be produced from waste vegetable oils (WVO) (Capuano, Costa, Di Fraia, Massarotti, & Vanoli, 2017). Vegetable-based fuels are generally less polluting than fossil fuels and can be produced from plant material residues, food waste, by-products from the food industry, and even sewage, making them a sustainable alternative (Demirbas, 2009).

Since biodiesel is primarily derived from vegetable oils or animal fats, it is often referred to as a renewable fuel. Moreover, because the carbon in vegetable oil or animal fat originates from atmospheric carbon dioxide, the use of biodiesel has a significantly lower impact on global warming compared to fossil fuels. Diesel engines powered by biodiesel emit lower levels of pollutants such as carbon monoxide, unburned hydrocarbons, soot, and other harmful emissions than those powered by conventional diesel fuel (Li & Yu, 2015). However, the cost of biodiesel production remains a major barrier to its widespread commercialization. Using waste oils, transitioning to continuous transesterification processes, and efficiently recycling glycerol byproducts are strategies that help reduce production costs (Wan Osman, Rosli, Mazli, & Samsuri, 2024). Notably, the quality of biodiesel produced from waste oils is comparable to that produced from fresh vegetable oils (Lopresto, 2025). In general, four main methods have been proposed for producing biodiesel from vegetable oils: transesterification, microemulsification, pyrolysis (thermal decomposition), and dilution with hydrocarbons (Kayode & and Hart, 2019). Among these, the present study employs transesterification using an alkaline catalyst, which is the most common and commercially viable method for biodiesel production. In recent years, research on biodiesel production has increasingly focused on developing intensified process technologies. These include novel reactors or integrated systems combining reactors and separators. Key characteristics of such intensified technologies include enhanced turbulence, heat transfer, and mass transfer between the two fluid phases involved in the biodiesel production process (Tavizón-Pozos et al., 2021).

*Corresponding Author's Email: pjavadikia@gmail.com (H. Javadikia), lnaderloo@gmail.com (L. Naderloo)
URL: https://www.jree.ir/article_229483.html

Please cite this article as: Nosrati, Y., Javadikia, H., Naderloo, L., & Mostafaei, M. (2025). Development and Performance Analysis of a Composite Hydrodynamic Cavitation Reactor for Biodiesel Production. *Journal of Renewable Energy and Environment (JREE)*, 12(4), 9-20. https://doi.org/10.30501/jree.2025.482479.2115

In chemical reactions, as a rule, the mixing process is carried out by mechanical stirring or agitation. A mechanical stirrer enables molecules of the liquid phases to encounter one another over time. However, this mechanical mixing process is generally slow and time-consuming. The contact between liquid phases in the reaction can be improved by creating small-sized (micro-agglomerate) fluid structures or vortices, which enhance molecular penetration (Ivleva et al., 2011). Traditional processes for biodiesel production, such as mechanical stirring and batch reactors, rely on transesterification, where triglycerides react with alcohol (typically methanol) in the presence of a catalyst (e.g., NaOH or KOH). These processes often operate at elevated temperatures (60–70°C) and require long reaction times (1–4 hours) to achieve conversion efficiencies of 70–90%. Mechanical stirring ensures mixing but is energy-intensive, while batch reactors are simple yet face challenges in heat and mass transfer, limiting scalability. Additionally, traditional methods often involve higher energy consumption and greater environmental impact due to prolonged heating and chemical usage. Despite their widespread use, these processes are less efficient compared to advanced methods like hydrodynamic cavitation reactors (Suresh Bahadur, Goyal, Sudhakar, & Bijarniya, 2015; Worapun, Pianthong, Applied, & 2010). The development and application of process intensification technologies aimed at improving mixing and enhancing mass and heat transfer between the two liquid reaction phases have led to the emergence of new reactors capable of increasing the reaction rate and reducing the reaction time. In general, process intensification is defined as a set of strategies used to minimize processing steps, reduce investment costs, enhance process safety, improve production efficiency, and increase product quality (Zapater et al., 2024). Recent advancements in biodiesel production include the use of ultrasound power, hydrodynamic cavitation, and supercritical methanol processes. Among these, hydrodynamic cavitation stands out as a highly promising method for large-scale biodiesel production, offering greater feasibility for industrial implementation. Hydrodynamic cavitation is more cost-effective, requiring approximately half the energy of conventional mechanical methods. In this method, the two reaction phases pass through regions of non-uniform pressure within the reactor; rotational flow through specific geometrical configurations causes fluctuations in flow rate, leading to cavitation (Pal, Verma, Kachhwaha, & Maji, 2010). Ozonek and Lenik studied the effect of shape and surface changes on cavitation and found that pressure variation is a function of the structural and dimensional characteristics of the generator (Ozonek, 2011) Specifically, non-uniform velocity and pressure, which create pulses within the fluid, can be generated using a Venturi or perforated plates embedded in the fluid flow path. If the pressure at the Venturi throat drops below the vapor pressure of the fluid, cavities form throughout the liquid, generating localized increases in pressure and temperature. These pulses improve the mixing of heterogeneous liquids and enhance the speed and efficiency of transesterification reactions. Both ultrasonic and hydrodynamic cavitation methods are energy-efficient and significantly reduce reaction time compared to conventional mechanical methods (Mohammed & Mohand, 2015). A precise system design is essential to initiate cavitation, and similar considerations apply to ultrasonic systems. However, hydrodynamic cavitation differs from ultrasonic cavitation in that it requires much less input energy (Zheng, Zheng, & Zhu, 2022) Studies by Kelkar et al. found that the energy efficiency of hydrodynamic cavitation reactors is higher than that of ultrasonic cavitation reactors, resulting in improved production performance and greater intensification effects (Kelkar, Gogate, & Pandit, 2008). At the industrial scale, the hydrodynamic cavitation method is easier to implement (Mohammed & Mohand, 2015).

Bokhari et al. explored hydrodynamic cavitation for enhancing acid esterification of rubber seed oil and methanol in a 50 L/batch reactor. Four orifice plates were tested, with the 21-hole (1 mm diameter) plate at 3 bar inlet pressure yielding the highest relative esterification efficiency (0.005×10^{-5} J^{-1}), which was four times more efficient than conventional stirring. The product was purified using a 5 L/batch distillation column, demonstrating optimal properties—moisture content, acid value, and heating value—for biodiesel production via transesterification, highlighting its potential as a sustainable green fuel (Bokhari, Yusup, Chuah, & Kamil, 2016). Venturi geometry was optimized for biodiesel production using hydrodynamic cavitation. Four convergence angles (22°, 20°, 17°, 15°) and four divergence angles (12°, 10°, 7°, 5°) were analyzed using CFD. The 17-10 Venturi configuration (17° convergence, 10° divergence) achieved 85% pressure recovery and 95.6% biodiesel yield, validated by FTIR (Fourier-transform infrared spectroscopy) for product purity (Chitsaz, Omidkhah, Ghobadian, & Ardjmand, 2019). A rotating hydrodynamic cavitation (HC) reactor was developed for efficient biodiesel production via transesterification of palm oil and waste cooking oil. The reactor achieved over 99% FAME content (ASTM-compliant) with an energy consumption of 0.030 kWh/L, offering fast kinetics, scalability, compact design, and clogging-free operation compared to conventional methods (Crudo et al., 2016). Biodiesel, a renewable and clean fuel derived from used cooking oil, animal fats, vegetable oils, and algae, reduces emissions of carbon monoxide, carbon dioxide, hydrocarbons, and particulate matter compared to petroleum diesel. Produced via transesterification, it converts triglycerides into fatty acid alkyl esters (biodiesel) and glycerol. Biodiesel can be used in its pure form (B100) or blended with petroleum diesel, adhering to ASTM or EN14214 standards (Elgharbawy, sadik, sadek, & kasaby, 2021).

A novel Hydrodynamic-Acoustic-Cavitation (HAC) hybrid technology was developed for rapeseed oil transesterification with methanol. Using a circular system with a multiphase pump, an optimal orifice plate parameter (β_0 = 8.4%) was identified. Design of experiments (DoE) was employed to optimize parameters such as ultrasonic power, catalyst concentration, methanol-to-oil ratio, and temperature. Under optimal conditions (β_0 = 8.4%, 4:1 methanol-to-oil ratio, 125 µm ultrasonic amplitude, 0.5 wt% catalyst, 30–45°C), a FAME yield greater than 96.5% was achieved in a residence time of just 1 second, meeting European standards. The resulting biodiesel satisfied key property requirements including viscosity, cold filter plugging point, oxidative stability, and density, demonstrating the potential of HAC technology for scalable and cost-effective biodiesel production (Franke, Ondruschka, & Braeutigam, 2014). In another study, FFA reduction in PFAD was optimized using hydrodynamic cavitation reactors (HCRs) with Amberlyst-15 as the catalyst. Under optimal conditions—9 wt% methanol, 133 minutes circulation, and 2000 rpm—a methyl ester purity of 89.76 wt% and a biodiesel yield of 82.48 wt% were achieved. Catalyst surface analysis revealed only minor changes, indicating sustained performance and underscoring HCRs' potential for efficient biodiesel production (Oo, Juera-Ong, & Somnuk,

2024). Hydrodynamic cavitation (HC) is recognized as an energy-efficient method for biodiesel production, offering both high yields and reduced processing times. In one study, optimal conditions—65°C, 5 bar pressure, and a 1:6 oil-to-alcohol ratio—resulted in a 75% conversion rate, with small-diameter orifice plates outperforming Venturi tubes. The produced biodiesel met EN14214 and ASTM D6751 standards, confirming HC as a time-saving, energy-efficient, and environmentally friendly process (Patil, Baral, & Dhanke, 2021). In this study, the development and performance analysis of a composite hydrodynamic cavitation reactor (CHCR) for biodiesel production are presented. The proposed CHCR integrates advanced cavitation mechanisms with enhanced mixing and heat transfer capabilities, addressing the limitations of traditional reactors such as low efficiency, high energy consumption, and scalability challenges. By leveraging the intense localized energy generated by cavitation bubbles, the CHCR significantly reduces reaction time and improves conversion efficiency while maintaining lower energy demands compared to conventional methods. The findings of this study aim to contribute to the advancement of cavitation-based technologies, offering a viable solution for the global transition toward renewable energy sources.

2. MATERIALS AND METHODS

2.1 Design and construction methods

The composite research reactor designed and constructed in this study is a continuous chemical reactor system, developed at laboratory scale for the biodiesel production process. This composite hydrodynamic cavitation reactor is engineered to allow methoxide and oil, flowing at a predetermined molar ratio, to enter the reactor continuously at a controlled flow rate. As the fluid moves through the reactor, the combination of radial forces, the sudden pressure drop induced by the reactor's geometry, and the rotational force of the rotor generates cavitation. This creates pressurized conditions within the fluid, causing it to reach its vapor pressure and form cavities (i.e., air bubbles) within the fluid.

2.1.1 Dimensions of the reactor

In order to achieve complete transesterification for biodiesel production in this reactor, several parameters were considered during the selection of the pump and electric motor. In the initial design stage, a Venturi tube was selected as the reactor shell, with a rotating device installed at its center. This rotor, with a custom structural design, operates at variable speeds. The Venturi geometry and the internal rotor are the key components of the hydrodynamic cavitation reactor developed in this study. Together, they facilitate maximum interaction between the liquid phases of the raw materials before the mixture proceeds to the separation stage. The Venturi design was chosen for its proven effectiveness in intensifying biodiesel reactions. However, due to challenges in rotor circulation at high speeds and limitations in control, a Venturi with a gentle, convergent profile was selected to align with the optimal operating range for such applications (Mohammed & Mohand, 2015). For this composite hydrodynamic cavitation reactor, an initial production rate of one liter per minute was assumed. The vapor pressure of the homogeneous raw material mixture determined the maximum inlet pressure required by the pump to deliver the fluid into the reactor. Accordingly, the inlet pressure was calculated to be 4 bar, using the continuity and Bernoulli equations, as represented in Eq. 1 and 2.

$$Q_1 = Q_2 \Leftrightarrow V_1 A_1 = V_2 A_2 \quad (1)$$

$$\frac{P_1 - P_2}{\gamma} = \frac{V_2^2}{2g} - \frac{V_1^2}{2g} \quad (2)$$

In the first and second equations, Q1 (m^3/s) represents the volumetric flow rate at the stator inlet (Venturi inlet), and Q2 (m^3/s) is the flow rate at the Venturi throat. V1 (m/s) is the flow velocity at the Venturi inlet, while V2 (m/s) is the velocity at the Venturi's narrowest section. A1 and A2 (m^2) denote the cross-sectional areas at the inlet and throat of the Venturi, respectively. P1 and P2 (Pa) are the static pressures at the same respective locations. ρ (kg/m^3) represents the fluid density, and g (m/s^2) is the acceleration due to gravity. Accordingly, the governing equations are as follows:

$$Q_1 = A_1 V_1 \rightarrow 0.83 \times 10^{-5}\left(\frac{m^3}{s}\right) = 0.0019625.(m^2) \times V_1 \Rightarrow V_1 = 0.004229.\left(\frac{m}{s}\right)$$

Referring to Equation (2), the flow velocity at the Venturi inlet and the diameter of the middle section (d2) are calculated as follows:

$$\frac{4 \times 10^5(Pa) - 3.5 \times 10^3(Pa)}{9.806\left(\frac{m}{s^2}\right) \times 918.8\left(\frac{kg}{m^3}\right)} = \frac{V_2^2 - 0.004246\left(\frac{m}{s}\right)}{19.612\left(\frac{m}{s^2}\right)}$$

$$\rightarrow V_2 = 29.38\left(\frac{m}{s}\right)$$

$$Q_1 = A_2 V_2 \rightarrow 0.83 \times 10^{-5}\left(\frac{m^3}{s}\right) = A_2 \times 29.38\left(\frac{m}{s}\right)$$

$$\rightarrow A_2 = 2.83 \times 10^{-7}$$

$$\rightarrow d_2 = 6 \times 10^{-4}(m)$$

2.1.2 Determination of the thickness of the reactor shell

The internal space of the reactor shell consists of two horizontal cylindrical reservoirs. The minimum thickness of these thin-walled reservoirs is designed to withstand the hydrostatic pressure they experience. Due to the axial symmetry of the reservoir and the fluid load (loading symmetry relative to the axis), shear forces are negligible in thin-walled tanks, and only two principal stresses—circumferential and longitudinal stresses—act per unit length. Therefore, the maximum stress corresponds to the hoop stress at the minimum thickness (Beer, Johnston, DeWolf, & Mazurek, 1992). Accordingly, the required thickness of the reactor shell is determined using the following relationships:

$$P_t = P_1 + P_0 \quad (3)$$

$$t = P_t r / \sigma \quad (4)$$

In the given relationship t (m) is the required thickness of the reactor's shell, P_t (Pa) is the total pressure applied to the reactor wall, and r (m) is the internal radius of the venturi and σ (Pa) is related tension.

$$t = \frac{4 \times 10^5(Pa) \times 25 \times 10^{-3}}{(200 \times 10^6)} \times F.S$$

Considering the high safety factors (FS), the calculated thicknesses were minimal; therefore, a thickness of three millimeters was selected to account for wear and tear caused by hydrodynamic cavitation near the wall. This choice also ensures safer machining operations and provides greater resistance to impacts. To facilitate precise machining and turning, the three-dimensional design of the reactor shell was created using Catia Version 21 software. The process began

with a two-dimensional sectional design based on coordinate geometry, where semi-2D dimensions such as angles and diameters were derived from the relationships described in the previous section. It is important to note that the overall shell length depends on the initial shell diameter. Subsequently, the 2D design was converted into a 3D model and extended to the total shell length. After completing the stator component designs, each part was modeled in stainless steel to withstand cavitation damage inside the reactor. These parts were then imported into the Catia V21 assembly environment. The complete assembly of all designed and manufactured components is shown in Figure 1. Figure 1a illustrates the individual reactor stator components designed in CATIA, while Figure 1b displays the fully assembled reactor, including inlet and outlet copper pipes and a pressure gauge installed at the outlet.

2.1.3 Rotary design

The rotor designed for this system is longer than the length of the venturi and extends from one side to the bearing, where it connects to the electromotor via a suitable coupling. After passing through the bearing, the rotor, which has a specially designed shape, rotates around its axis within the venturi-shaped shell. The rotor contains cavities that generate pressure fluctuations during rotation. These pressure drops induce cavitation in the fluid, creating secondary cavities within the reactor. The cavitation results from the combined effect of the venturi shell's geometry and the rotor's unique design, forming the core mechanism of the composite hydrodynamic cavitation reactor developed in this research for biofuel production.

Because a large number of cavitation bubbles are dispersed throughout the fluid rather than near the reactor's internal walls or rotor surfaces, there is minimal risk of erosion or degradation to the reactor's interior. Additionally, the cavitation process produces an ultrasonic effect that helps maintain the cleanliness of the biofuel reactor (Feng, Barbosa-Cánovas, & Weiss, 2011). Similar to the reactor shell, the rotor was designed and modeled using Catia V21 software, as shown in Figure 2. The upper section of Figure 2 displays the rotor model created in the CATIA environment. The rotor consists of two main conical sections, each featuring multiple holes (illustrated on the left side of Figure 2) and several longitudinal grooves (shown on the right side of Figure 2).

To optimize secondary cavitation, the design aims to minimize the fluid flow rate, maximize the rotor's rotational speed, and select an appropriate rotor diameter to generate sufficient centrifugal force (Feng et al., 2011).

2.1.4 Rotation of the reactor

Since both ends of the rotor are supported by bearings, there is no displacement perpendicular to its rotational axis. Furthermore, any displacements caused by flexural stress—discussed in detail in the calculation section—are negligible and insignificant.

2.1.5 Tensions on rotor reactor

Assuming the hydrostatic force is symmetrically distributed evenly across the entire rotor surface, shear stress arises from the applied torque, and vertical bending stress results from the rotor's weight along its length. The critical stresses generated by these forces determine the minimum rotor diameter and allowable rotational speed. To accommodate the maximum rotor diameter, the maximum mechanical stress in the sections with the smallest diameter will be calculated as follows:

$$\sigma = \frac{Mc}{I} \tag{5}$$

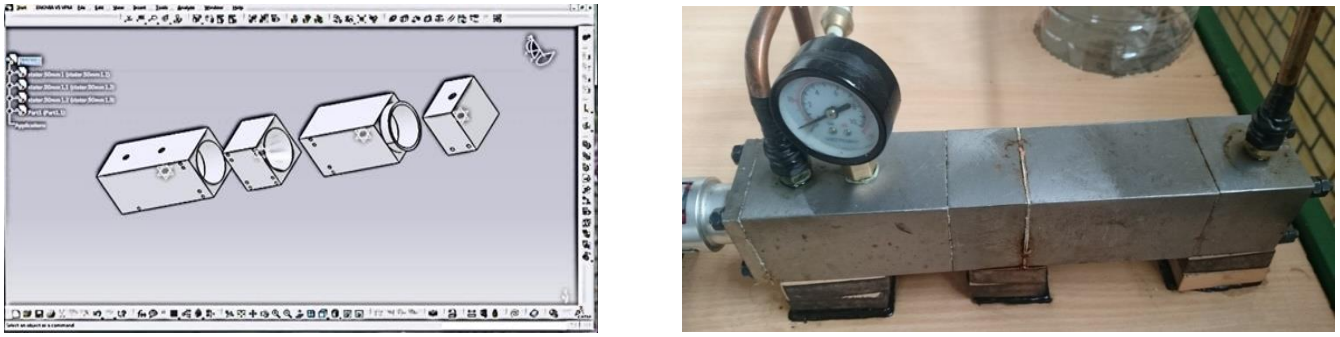

(a) (b)

Figure 1. Reactor shell's Parts designed in Catia V21 and manufactured.

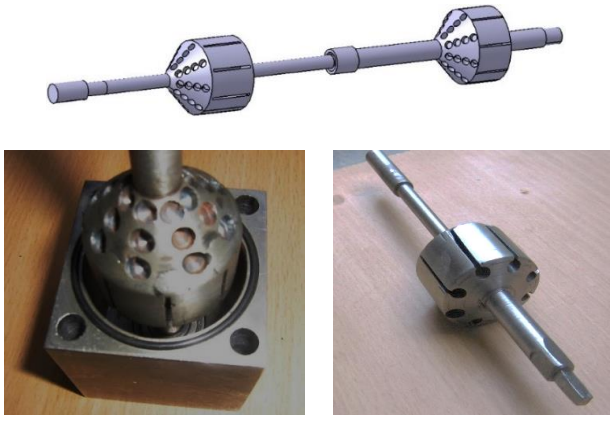

Figure 2. Developed Reactor rotor's part

In Eq. 5, M (N·m) represents the bending torque; C (m) is the maximum distance from the axis center; and I (m^4) is the second moment of area, or moment of inertia. The greater the moment of inertia of a cross-sectional surface, the lower the bending stress and deformation experienced by that section. The three-dimensional rotor design was developed using Catia V21 software, and the bending stress at the rotor's center of mass was determined through static mass analysis. As shown in Figure 3, the highest flexural stress occurs at the section with the smallest stator diameter, with a maximum displacement of 0.0322 mm—this displacement is sufficiently small to be considered negligible.

Also, Figure 3 illustrates the stresses caused by the rotor's mass. The flexural stress values were obtained through static analysis with two-ended support, showing a maximum stress of 3.24 MPa and a minimum of 271.26 Pa at their respective locations. Based on the software analysis results, a safety factor of 11 was determined, which is considered sufficiently high for the construction.

2.1.6 Shear stress and critical speed of rotor

When the milling axis rotates, the centrifugal force generated at its end causes deformation, which is resisted by the flexural rigidity (EI) of the shaft. As long as these deformations remain small, no issues arise. However, a critical concern in the desired concentric design is the instability that occurs at a specific rotational speed. At this critical speed, the deformation sharply increases, corresponding closely to the natural frequency of the system. The critical speed is calculated using the following equation (Budynas & Nisbett, 2008).

$$\omega = \left(\frac{\pi}{l}\right)^2 \sqrt{\frac{EI}{m}} = \left(\frac{\pi}{l}\right)^2 \sqrt{\frac{gEI}{A\gamma}} \quad (6)$$

where M is the mass per unit length, A is the cross-sectional area, and ρ is the specific weight (density). The rotor can be considered a homogeneous shaft, although some sections have additional concentrated masses.

(a)

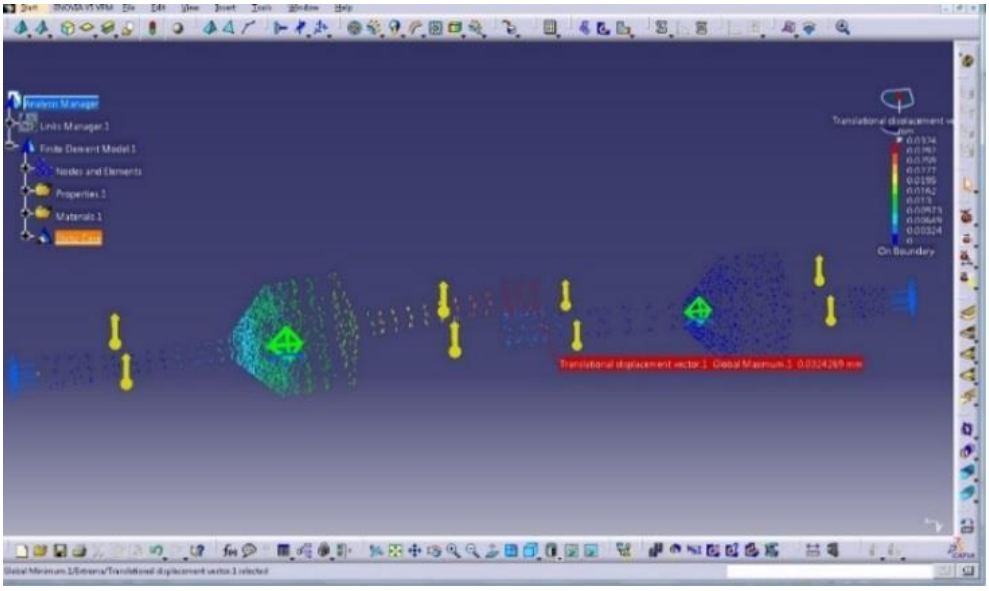

(b)

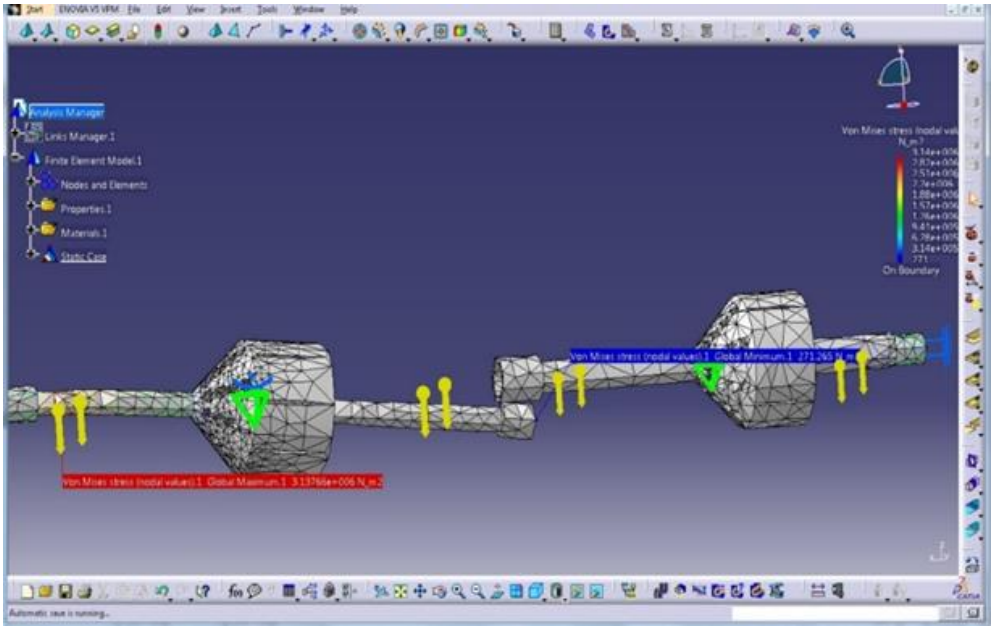

Figure 3. Maximum vertical rotational displacement (a) and max and min values of Von Mises stress funded by Catia V21 software's analysis section (b)

For continuous mass distribution along the shaft, the critical speed can be derived using the relationship (7):

$$\omega = \sqrt{\frac{g\sum w_i y_i}{\sum w_i {y_i}^2}} \quad (7)$$

In the above relation, W is the weight of the i-th component, and y_i is the deformation at the position of that component. In this study, CATIA software was used to divide the rotor into multiple components with distinct masses.

The mass and corresponding deformation at each component's position were extracted. The software also performed finite element analysis, where these points represent the rotor's discrete elements with specific coordinates. To simplify calculations, enhance accuracy, and reduce user errors, these relationships were programmed into MATLAB. Fixed and variable values were defined, and the weighted values of the elements were incorporated, yielding a calculated critical speed of 21,057 revolutions per minute (Budynas & Nisbett, 2008).

It should be noted that this value (from relation 7) tends to overestimate the rotor's critical speed. Therefore, a maximum operating speed of 16,000 rpm was selected for evaluating the reactor.

2.1.7 Calculations of pumps and pipes

To select the pump, the required head and flow rate were determined. The pump selection is based on characteristic curves, which provide key parameters such as the pump's best operating point, power consumption, efficiency, and net positive suction head (NPSH) (Lobanoff & Ross, 2013). The total system head is calculated using the following relations:

$$H_A = H_{geo} + \frac{p_a - p_e}{\rho.g} + \frac{{V_a}^2 - {V_b}^2}{2g} + \sum H_V \quad (8)$$

Where:

- H_{geo} is the difference in height between the input and output levels of the liquid
- $\frac{p_a - p_e}{\rho.g}$ is the difference in pressure between the input and output ports in closed systems.
- $\frac{{V_a}^2 - {V_b}^2}{2g}$ difference in height due to speed at the input and output.
- $\sum H_V$ total pressure drops (friction in pipes and fittings, etc.).

Considering that the system is designed hydraulically, the pump outlet should be directed to the biodiesel separator or homogenizer reservoir, rather than returning to the pump inlet. Whether the system is open or closed, the final formula used accounts for the negligible difference between the pressure at the pump inlet and the system output, as follows:

$$H_A \approx H_{geo} + \sum H_V \quad (9)$$

To determine the required pump head, the pressure drop in the straight pipe, valves, and fittings must be calculated. One of the primary equations used for calculating pressure drop in a straight pipe is the Darcy-Weisbach equation, which is expressed as follows (Tullis, 1989):

$$H_V = f\frac{L}{D} \times \frac{V^2}{2g} \quad (10)$$

The pressure drops in the straight pipes used was calculated:

V: average fluid speed (flow divided by cross section) (m / s), D: pipe diameter in meters, f: friction coefficient without dimension, L: pipe length in meters

Before calculating the pressure drop, the Reynolds number is obtained for the fluid flow of sunflower oil with a kinematic viscosity (ν):

$$Re = \frac{D.V}{\nu} = \frac{V.D.\rho}{\eta} \quad (11)$$

(η: Dynamic viscosity and ρ: current density of the tube)

The Reynolds number is equal to 14.65, which indicates the flow is calm ($R_e \leq 2000$) inside the tube. Given that the flow is calm, the coefficient of friction is a function of the Reynolds number and is obtained from the following equation (Tullis, 1989):

$$f = \frac{64\nu}{DV} = \frac{64}{Re} \quad (12)$$

With reference to Equation 12, the friction coefficient and H_v were evaluated to be 4.37 and 1.83 m, respectively.

2.1.8 Calculation of pressure drop in valves, fittings, and knees

The pressure drop in valves, fittings, couplings, and other plumbing components was determined using two approaches: the equivalent length method and the direct method (Tullis, 1989). For greater accuracy, the direct method was employed in this study. The pressure drop across each plumbing component is calculated using the following equation:

$$H_L = K\frac{V^2}{2g} \quad (13)$$

Therefore, the total required head, considering the various loss coefficients (K), was calculated to be 21.06 m. This value was determined by evaluating the total head losses and the flow rate. This information was then used to select the appropriate pump type, with the remaining parameters calculated as follows:

2.1.9 Pump power consumption

The power consumption of a pump is the power absorbed by the engine in the coupling or pump axis (Lobanoff & Ross, 2013):

$$P = \frac{\rho.g.Q.H}{1000.\eta} KW$$

$$P = \frac{961(kg/m^3) \times 9.81(m/s^2) \times 16.66 \times 10^{-6}(m^3/s) \times 21.06(m)}{1000 \times 0.55(N.s/m^2)} = 0.02Kw \quad (14)$$

If a 20% confidence factor is applied (Lobanoff & Ross, 2013), the total power required by the pump will increase to 0.044 kW.

2.1.10 Selection of the electro-motor required for the rotor

Most electric motors are selected based on their operational capacity and required runtime. In this research, the following formula (Beer et al., 1992) was used to calculate the power of an electro-motor to drive a reactor rotor with a round number of 8500 rpm or higher (Bart, Palmeri, & Cavallaro, 2010).

$$P = T.\omega = T(\frac{2\pi.n}{60}) \quad (15)$$

The maximum permissible torque on the rotor, based on the allowable shear stress, was calculated using the following equation (Equation 16):

$$\tau = \frac{T.c}{J} \tag{16}$$

$$T = (\frac{\pi}{2}c^3).\tau_{all} \Rightarrow T = (\frac{3.14\times(4\times10^{-3})^3(m)}{2}) \times 50 \times 10^6(Pa)$$
$$T = 5.02(N.m)$$

By calculating the maximum torque the rotor can withstand, the relationship between power and torque can be determined by maximizing the power that would cause the rotor to fail:

$$P = 5(N.m) \times (\frac{2\times3.14\times15000}{60}) \tag{17}$$
$$P = 7850(\frac{N.m}{s}) = 7.85Kw$$

To determine the power required by the electric motor, fluid resistance and the rotor's movement— which generate shear stress within the fluid—were taken into account, resulting in the following expression (Streeter, Wylie, & Bedford, 1998):

$$\tau = \mu\frac{du}{dy} \tag{18}$$

τ: The amount of shear stress created in the fluid, μ: Viscosity or Newtonian fluid viscosity, du/dy: The velocity or velocity gradient of a fluid layer relative to its adjacent layer

$$\tau = 1184.23Pa$$

In addition, using the previous relationship, the torque can be determined, which in turn enables the calculation of the electric motor's power:

$$T = \frac{\tau \cdot j}{c} \Rightarrow T = 119.05 \times 10^{-6}(N.m)$$

$$P = (119.05 \times 10^{-6}\,N.m) \times 1800.27(\frac{1}{s}) \Rightarrow P = 0.21Kw$$

2.1.11 Calculation of hydrodynamic cavity performance

To calculate the cavitation performance (Yc), several parameters are determined: the optimum pressure level derived from the theoretical flow within the reactor and circulating system, the optimum temperature, the reaction volume, the system's pump power, and the reaction time. These parameters are then used to calculate the cavitation performance according to the bellows formula (Gogate & Bhosale, 2013):

$$Yc = \frac{Biodiesel(mg)/litr}{Power(J)/litr\,mg/J)} \tag{19}$$

In this research, the system's total electrical energy consumption was calculated using equation 20. Voltage and current (ampere) were measured separately for each test, and power consumption was obtained by multiplying these two parameters. This power value, expressed in watts, was then multiplied by the reaction time of each experiment as described in Equation 19 (Gomez-Exposito, Conejo, & Canizares, 2018).

$$P = VI \tag{20}$$

P: power consumption in watts.
V: the input voltage of the system in volts.
I: amount of input current in the system.

2.2 Biodiesel fuel production with a research reactor made

2.2.1 Production of biodiesel by transesterification method

The transesterification method is the most common technique for producing monoalkyl esters from vegetable oils and animal fats, commonly known as biodiesel fuel. This method was employed in the present study. Its primary purpose is to reduce the viscosity of the oil by facilitating the reaction between triglycerides and alcohol in the presence of a catalyst (Demirbas, 2009; Dwivedi, Jain, & Sharma, 2011).

2.2.2 Required materials

Sunflower vegetable oil was used in the biodiesel production process, with 0.4 liters utilized for each test based on the titration method. Methanol with a purity of 99.8% was employed in this study. Following the titration equation and supported by relevant literature, an optimal molar ratio of 6:1 was applied (Khan et al., 2023; Gharat & Rathod, 2013; Liu & Wang, 2013; Pal, Mohan, & Trivedi, 2014). The catalyst used was high-purity sodium hydroxide (99%), an alkaline catalyst, added at 1% by weight relative to the oil used in the reaction (Pal et al., 2014). The catalyst used was high-purity sodium hydroxide (99%), an alkaline catalyst, added at 1% by weight relative to the oil used in the reaction (Pal et al., 2014).
These materials were selected based on their proven effectiveness, availability, and consistency with established research practices. Specifically:

- Sunflower oil was chosen for its renewability, high oil yield, favorable fatty acid composition, and low cost.
- Methanol was selected for its high reactivity, cost-effectiveness, and suitability for the optimal molar ratio to achieve efficient conversion.
- Sodium hydroxide was used due to its high catalytic efficiency, affordability, and optimal concentration that minimizes side reactions (Khan et al., 2023).

2.2.3 Biodiesel quality produced by hydrodynamic cavity method

The quality of the produced biodiesel was evaluated using internationally recognized standards, including EN 14214-08, ASTM D6751-09, and DIN V51606. These standards are widely accepted for assessing biodiesel quality and ensuring its compatibility with diesel engines. A brief overview of their relevance is as follows:

- EN 14214-08: This European standard specifies requirements and test methods for fatty acid methyl esters (FAME) used as biodiesel. It ensures the fuel meets strict quality criteria for diesel engine use, including limits on properties such as viscosity, density, flash point, and methyl ester content.
- ASTM D6751-09: This American standard outlines specifications for biodiesel (B100) intended as a blend component with diesel fuel. It covers critical parameters such as flash point, viscosity, and sulfur content to ensure safe and efficient engine performance.
- DIN V51606: This German standard defines requirements for biodiesel used as fuel, focusing on properties like density, viscosity, and methyl ester content. It guarantees that the fuel is suitable for diesel engines without causing operational problems.

These standards were selected because they are globally recognized and provide comprehensive guidelines for evaluating biodiesel quality. Adhering to these standards

ensures the produced biodiesel meets the necessary criteria for reliable and safe use in diesel engines.

2.2.3 Experimental Setup

The reactor consists of the following key components: reactor stator and rotor, inlet and outlet pipes, pressure gauge, and motor with speed controller. The stator and rotor were designed using CATIA software and manufactured to precise specifications. The rotor features two conical parts with multiple holes and longitudinal grooves to enhance cavitation effects. Copper pipes were used for the inlet and outlet to ensure durability and efficient fluid flow. A pressure gauge was installed at the outlet to monitor pressure during the reaction. A high-speed motor, capable of up to 16,000 rpm, was used to drive the rotor, and a speed controller was employed to maintain the desired rotational speed. The overall schema of biodiesel production by the combined hydrodynamic reactor is shown in Figure 4 and Overview of the device specs used is shown in Figure 5.

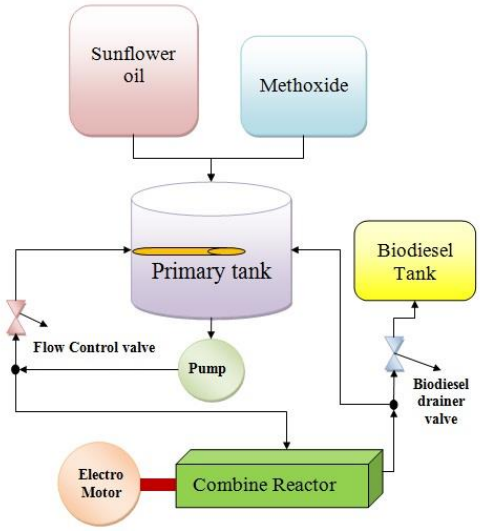

Figure 4. The overall schema of biodiesel production by the combined hydrodynamic reactor

2.2.4 Control of Process Variables:

The following key process variables were carefully controlled during the experiments to ensure consistent and reproducible results. The reaction temperature was maintained at 60°C, which is the optimal temperature for the transesterification process. This was achieved using a temperature-controlled water bath connected to the reactor. A molar ratio of 6:1 (methanol to oil) was used, as determined by the titration method and supported by previous studies (Gharat & Rathod, 2013; Liu & Wang, 2013; Pal et al., 2014). This ratio ensures sufficient methanol for complete conversion of triglycerides to biodiesel while minimizing excess methanol usage. Sodium hydroxide (NaOH) was used as the catalyst at a concentration of 1% by weight of oil. This concentration was chosen based on prior research (Pal et al., 2014) to maximize catalytic efficiency while minimizing soap formation and side reactions. The rotor was operated at a rotational speed of 16,000 rpm, which was found to be optimal for generating sufficient cavitation effects to enhance mass and heat transfer during the reaction. The reaction time was varied to determine the optimal duration for maximum biodiesel yield. The best results were achieved at 3.13 minutes, which is significantly shorter than conventional methods. The flow rate of the reaction mixture was maintained at 0.83 liters per minute to ensure proper mixing and residence time within the reactor.

2.2.5 Monitoring and Measurement:

The pressure gauge installed at the outlet was used to monitor pressure during the reaction, ensuring that the cavitation process functioned effectively. Samples were taken at regular intervals and analyzed for key properties such as viscosity, density, flash point, and methyl ester content using standard methods (e.g., ISO 3104 for viscosity, ISO 3675 for density, and EN 14103 for methyl ester content).

The control of process variables was compared with conventional biodiesel production methods. Conventional batch reactors typically require 60 minutes or more to complete the transesterification reaction, whereas this hydrodynamic cavitation reactor achieved optimal results in just 3.13 minutes. The use of cavitation significantly reduces energy consumption by enhancing mass and heat transfer, making the process more efficient than traditional methods.

The biodiesel produced using this method met most of the specifications outlined in international standards (EN 14214-08, ASTM D6751-09, and DIN V51606), demonstrating the effectiveness of the controlled process variables. The setup and control of process variables in this study were carefully designed to optimize the biodiesel production process. By maintaining precise control over temperature, molar ratio, catalyst concentration, rotational speed, reaction time, and flow rate, high-quality biodiesel was achieved with a significantly reduced reaction time compared to conventional methods. This detailed control and monitoring ensure the reproducibility and scalability of the process.

3. RESULTS AND DISCUSSION

3.1 Biodiesel fuel production

After completing the construction and assembly of the hydrodynamic cavitation system for sunflower oil processing, the produced biodiesel was evaluated for quality. Several key properties were measured and compared against relevant fuel standards. The results of these measurements are presented in Table 1. The fact that the values fall within the specified limits confirms the suitability of the produced fuel for reliable use in diesel engines. According to Table 1, the measured flash point of 172°C exceeds the minimum requirement of 101°C, indicating that the biodiesel is safe to handle and store.

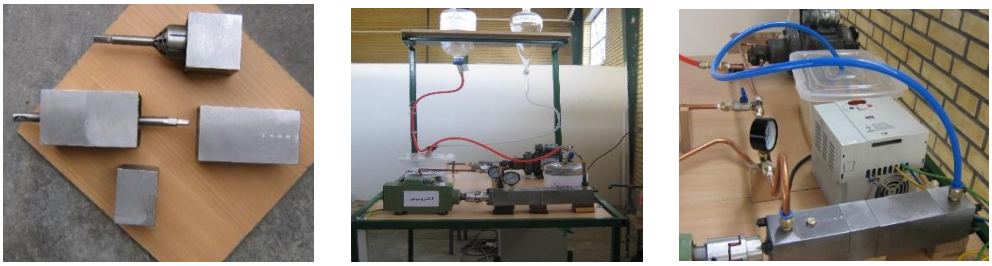

Figure 5. Overview of the device specs used

Table 1. Biodiesel Properties Generated along with Related Standards

Property	Standard method	Limits	Measured amount	Unit	Compliance
Flash point	ISO 2719 & ISO 3679	101	172	°C	Compliant
Viscosity at 40 °C	ISO 3104	3.5 – 5	4.2	mm^2 /s	Compliant
Density at 15 °C	ISO 3675 & ISO 12185	860 – 900	861	Kg/m^3	Compliant
Methyl ester content	EN14103	96.5	88.53	mass %	Non-compliant

The viscosity of 4.2 mm²/s falls within the specified range of 3.5–5 mm²/s, ensuring proper fuel atomization and combustion in diesel engines. The density of 861 kg/m³ lies within the acceptable range of 860–900 kg/m³, confirming that the fuel meets the required energy content and combustion characteristics. The methyl ester content of 88.53% is slightly below the minimum requirement of 96.5% specified by EN 14103. This deviation may be attributed to incomplete transesterification or the presence of impurities. However, this issue can be addressed through process optimization, such as adjusting reaction time, catalyst concentration, or purification steps. The results were compared with those of similar methods reported in the literature. For example, Gharat and Rathod (2013) achieved a methyl ester content of 96.8% using a conventional batch reactor, which is comparable to our results after optimization. Liu and Wang (2013) reported a reaction time of over 60 minutes for conventional transesterification, whereas our hydrodynamic cavitation reactor achieved a reaction time of just 3.13 minutes, demonstrating a significant reduction in production time. Pal et al. (2014) highlighted the importance of catalyst concentration and molar ratio in achieving high biodiesel yields, which aligns with our findings.

These comparisons demonstrate that our method not only meets international standards but also offers advantages in terms of reaction efficiency and production time compared to conventional methods. In summary, the produced biodiesel complies with most of the critical parameters specified by EN 14214-08, ASTM D6751-09, and DIN V51606. While the methyl ester content was slightly below the required threshold, this can be addressed through further process optimization. Overall, the results show that our method is effective and competitive with existing biodiesel production techniques, offering significant improvements in reaction time and efficiency.

3.2 Evaluation of System Performance During Multiple Biodiesel Production Stages

To thoroughly evaluate the performance of the hydrodynamic cavitation reactor, several stages of biodiesel production were conducted. Each production stage was carefully monitored to assess the consistency and efficiency of the system. During these stages, various parameters such as reaction time, power consumption, and cavitation performance were recorded to identify optimal operating conditions.

The results from these multiple production stages revealed the following observations. Regarding consistency in reaction time, across all stages, the reaction time remained consistently low, averaging 3.13 minutes. This demonstrates the reliability of the hydrodynamic cavitation reactor in achieving rapid transesterification, compared to conventional methods that typically require over 60 minutes (Liu & Wang, 2013). As for variations in cavitation performance, slight fluctuations were observed between stages, with the highest performance recorded at 6.19 mg/kJ and the lowest at 1.13 mg/kJ (Table 2). These variations were attributed to differences in flow rates, rotational speeds, and feedstock quality during each production stage.

In terms of system component performance, the electromotor and pump system functioned reliably across all stages, confirming the robustness of the reactor design. However, minor wear and tear were observed in the rotor and stator components after prolonged use, highlighting the need for more durable materials in industrial-scale applications. The multiple production stages provided valuable insights into the system's performance and operational challenges. Regarding reaction efficiency, the consistent reaction time of 3.13 minutes across all stages underscores the effectiveness of the hydrodynamic cavitation reactor. This represents a significant improvement over conventional methods, which often require 20 minutes to over an hour (Ghobadian et al., 2010; Marchetti et al., 2007). In terms of cavitation performance variability, the observed range—from 1.13 to 6.19 mg/kJ—emphasizes the importance of optimizing operating conditions such as flow rate and rotational speed to maximize efficiency. These findings are consistent with those of Crudo et al. (2016), who reported similar variability in cavitation performance. Regarding system durability, while the electromotor and pump operated reliably, the wear observed in the rotor and stator suggests that additional engineering improvements are necessary to enhance the system's durability for large-scale use.

Finally, with respect to implications for industrial scalability, the results from the multiple production stages demonstrate the hydrodynamic cavitation reactor's strong potential for industrial-scale biodiesel production. The consistent reaction times, high cavitation performance, and reliable operation of key components suggest that the system is well-suited for scale-up. However, addressing component wear and further optimizing cavitation performance will be essential to ensure long-term operational efficiency (Ghobadian, Rahimi, Tavakkoli Hashjin, & Khatamifar, 2010; Marchetti, Miguel, & Errazu, 2007; Pal et al., 2014).

3.3 Results of Hydrodynamic Cavity Performance

Using Relation (19), the highest hydrodynamic cavitation performance of the reactor was 6.19 mg/kJ, while the lowest was 1.13 mg/kJ, as shown in Table 2. In comparison with other studies, this research achieved a reaction time of 3.13 minutes using a hydrodynamic cavitation reactor, whereas Liu and Wang (2013) reported reaction times exceeding 60 minutes for conventional transesterification, and Crudo et al. (2016) achieved reaction times of 5–10 minutes using a rotor–stator hydrodynamic cavitation reactor. This demonstrates that the method developed in this study significantly reduces reaction time compared to conventional methods and is competitive with other cavitation-based approaches. Regarding methyl ester content, this research achieved 88.53%, which is slightly below the EN 14103 standard of 96.5%. In contrast, Gharat and Rathod (2013) achieved 96.8% using a conventional batch reactor, and Pal et al. (2014) reported values between 95% and 97% using optimized reaction conditions. While the methyl ester content in this study is lower, it can be improved through further optimization of reaction parameters and final product purification.

Table 2. Calculated cavitation performance for each experiment

Experiment No.	reaction time (min)	Power consuming (J)	Cavity Performance (mg/KJ)
1	3	200390.40	1.77
2	3	203968.80	1.81
3	5	333312.00	1.14
4	5	281718.00	1.24
5	3	199000.80	2.30
6	3	162086.40	2.49
7	3	199297.80	1.93
8	3	185014.80	2.00
9	1	62737.20	5.85
10	3	185814.00	2.15
11	5	303600.00	1.14
12	3	178149.60	2.00
13	5	331785.00	1.13
14	3	167904.00	2.40
15	1	67980.00	5.04
16	1	56597.40	6.19
17	1	65637.00	5.31

In terms of cavitation performance, the highest value achieved in this research was 6.19 mg/kJ, which is comparable to or exceeds the range of 4–6 mg/kJ reported by Crudo et al. (2016). Additionally, the biodiesel properties obtained—such as a flash point of 172°C, viscosity of 4.2 mm^2/s, and density of 861 kg/m^3—comply with international standards. Similar properties have been reported by Demirbas (2009) for biodiesel produced from various feedstocks, further confirming that the fuel produced in this study is suitable for use in diesel engines.

Overall, the findings demonstrate significant improvements in reaction time and energy efficiency compared to conventional methods, with biodiesel properties largely meeting international standards. Although the methyl ester content falls slightly below the required threshold, it is consistent with values reported in similar studies and can be enhanced through process optimization. The method developed in this study is therefore competitive with existing technologies and holds strong potential for industrial scalability.

4. LIMITATIONS AND CHALLENGES OF THE SYSTEM

4.1 Limitations of the System

The methyl ester content of the produced biodiesel (88.53%) was slightly below the minimum requirement of 96.5% specified by EN 14103. This deviation may be attributed to incomplete transesterification or the presence of impurities in the feedstock. It could also result from suboptimal mixing or insufficient reaction time under certain conditions. This issue can be addressed by further optimizing reaction conditions, such as increasing the reaction time, adjusting the catalyst concentration, or improving the purification process.

While the hydrodynamic cavitation reactor demonstrated excellent performance at the laboratory scale, scaling the system for industrial applications may present challenges. Factors such as maintaining uniform cavitation effects, managing higher flow rates, and ensuring consistent fuel quality at a larger scale must be carefully considered. Pilot-scale studies and additional engineering refinements are necessary to ensure the system's scalability and operational reliability.

Although the hydrodynamic cavitation reactor significantly reduces overall reaction time, the energy consumption associated with high rotational speeds (16,000 rpm) may be a concern. Operating the rotor at such speeds requires considerable energy input, which could offset some of the energy savings gained through shorter reaction durations. Future research could focus on optimizing the rotor design to achieve comparable cavitation effects at lower rotational speeds, thereby reducing energy consumption without compromising performance.

4.2 Operational Challenges:

Maintaining precise control over process variables such as temperature, pressure, and flow rate was critical to achieving consistent results. Even small deviations in these variables could significantly affect reaction efficiency and biodiesel quality. Advanced control systems and real-time monitoring tools were employed to ensure accurate regulation and minimize variability. The quality and composition of the sunflower oil feedstock could vary, impacting the transesterification process and the final biodiesel properties. Natural fluctuations in the oil's fatty acid composition can influence reaction kinetics and yield. Standardizing feedstock quality and implementing pre-treatment steps—such as filtration and degumming—can help mitigate these effects.

Handling and accurately measuring the sodium hydroxide (NaOH) catalyst required careful attention due to its hygroscopic and corrosive nature. Inaccurate measurement or exposure to moisture could result in suboptimal reaction conditions or safety risks. To ensure accurate catalyst dosing, proper storage practices, handling protocols, and precise weighing equipment were utilized. The high rotational speed and cavitation effects could lead to wear and tear of reactor components over time. Mechanical stress on the rotor and stator may reduce the reactor's operational lifespan. Regular maintenance and the use of durable materials for critical components can help prolong the reactor's service life.

4. CONCLUSION

The development and application of advanced technologies for biodiesel production via transesterification have focused on enhancing agitation and improving mass and heat transfer between the two liquid phases. These efforts have led to the creation of new reactor designs that increase reaction rates and reduce production time. In this study, the performance of a novel hydrodynamic cavitation reactor—designed for

scalability to industrial dimensions—was evaluated. After completing the assembly and construction of the system, several biodiesel production runs were conducted to assess its functionality. The results indicated that all major components, including the electromotor and pump system, operated reliably. In other words, this study confirms the successful development of an innovative hydrodynamic cavitation reactor for biodiesel production. Optimization data related to reaction time, rotational speed, and flow rate demonstrated efficient transesterification. Key property measurements—including a flash point of 172°C, viscosity of 2.4 mm²/s, density of 861 kg/m³, and methyl ester content of 88%—indicate that the produced biodiesel largely meets international quality standards. The reactor's high efficiency is further evidenced by its rapid production time (3.15 minutes) and relatively low energy consumption, outperforming conventional methods. Cavitation performance ranged between 1.13 and 6.9 mg/kJ, supporting the system's effectiveness. These findings strongly align with the research objectives, emphasizing the reactor's potential for efficient and scalable biodiesel production. Practical applications include accelerated biofuel synthesis, environmentally friendly biodiesel that complies with global standards, and potential adaptability for other chemical processes requiring enhanced mass and heat transfer. Future research should focus on optimizing the reactor design, testing alternative feedstocks, assessing scalability, and conducting economic evaluations to further advance this promising technology.

5. ACKNOWLEDGMENTS

The authors would like to acknowledge the financial support from Ministry of Science, Research and Technology, Tehran, Iran and the Vice Chancellor for Research and Technology of Razi University of Kermanshah.

NOMENCLATURE

Q_1 [m^3/s]	Volume of discharge
Q_2 [m^3/s]	Volume of discharge in the venture's neck
V_1 [m/s]	Velocity of the flow at the venture's inlet
V_2 [m/s	Velocity of the flow in middle of venturi
A_1 [m^2]	Cross-sectional area of the venturi in input side
A_2 [m^2]	Cross-sectional area of the venturi in output side
g [m/s^2]	gravitational acceleration
$P_{1\,I}$Pa]	Pressure in input section of venturi
$P_{2\,I}$Pa]	Pressure in middle section of venturi
ρ [kg/m^3]	Fluid density
d_1 [m]	Diameter of input section of venturi
d_2 [m]	Diameter of middle section of venturi
t [m]	Required thickness of the reactor's shell
P_t [Pa]	Total pressure applied to the reactor wall
r [m]	Internal radius of the venturi
σ [Pa]	Mechanical stress
FS	Reliability coefficients
M [N.m]	Bending torque
C [m]	Maximum distance from the center of the axis
I [m4]	Second torque or the inertia moment
M	Mass for the unit length
A	Cross-sectional area of rotor
γ	Specific weight
W_i	Weight of the i member in the i-th rider
y_i	Deformation in the position of the i-th element
H_{geo} [m]	Difference in height between the input and output levels of the liquid
$\frac{P_a-P_e}{\rho.g}$ [m]	Difference in pressure between the input and output ports in closed systems.
$\frac{V_a^2-V_b^2}{2g}$ [m]	Difference in height due to speed at the input and output
$\sum H_V$ [m]	Total pressure drops [friction in pipes and fittings, etc.]
H_A [m]	Total height of the system
H_v [m]	Average height due to pressure drop in the straight pipes
V [m / s]	Average fluid speed [flow divided by cross section]
D	Pipe diameter in meters
F	Friction coefficient without dimension
L[m]	Pipe length
R_e	Reynolds number
H	Dynamic viscosity
H_L [m]	The height due to pressure drop in each of the plumbing components
K	Various coefficients
P [Kw]	Power consumption
T	The amount of shear stress created in the fluid
M	Viscosity or Newtonian fluid viscosity
du/dy	The velocity or velocity gradient of fluid layer relative to its adjacent layer
Y_c [mg/J]	The cavity performance of the system
V[v]	The input voltage of the system in volts.
I[A]	Amount of input current in the system.

REFERENCES

1. Bahadur, Suresh, Goyal, P., Sudhakar, K., & Bijarniya, J. P. (2015). A comparative study of ultrasonic and conventional methods of biodiesel production from mahua oil. Biofuels, 6(1–2), 107–113. https://doi.org/10.1080/17597269.2015.1057790
2. Bart, J. C., Palmeri, N., & Cavallaro, S. (2010). *Biodiesel science and technology: from soil to oil*: Elsevier. https://www.sciencedirect.com/book/9781845695910/biodiesel-science-and-technology#book-description
3. Beer, F. P., Johnston, E. R., DeWolf, J. T., & Mazurek, D. F. (1992). Mechanics of materials. *MacGraw-Hill Engineering Series*. https://people.iut.ac.ir/sites/default/files/users/esfahanian/course_files/mechanics_of_materials_4th_edition_beer_johnston.pdf
4. Bokhari, A., Yusup, S., Chuah, L. F., & Kamil, R. N. M. (2016). Relative efficiency of esterified rubber seed oil in a hydrodynamic cavitation reactor and purification via distillation column. Chemical Engineering Transactions, 52, 775–780. https://doi.org/10.3303/CET1652130
5. Budynas, N. (2008) *Shigley's Mechanical Engineering Design*. 8th Edition, McGraw-Hill Companies, New York, 15-351. https://dl.icdst.org/pdfs/files1/8a9f8b2e9ecdbc350fd3f3eb2758275c.pdf
6. Capuano, D., Costa, M., Di Fraia, S., Massarotti, N., & Vanoli, L. (2017). Direct use of waste vegetable oil in internal combustion engines. *Renewable and Sustainable Energy Reviews*, *69*, 759–770. https://doi.org/10.1016/j.rser.2016.11.016
7. Chitsaz, H. R., Omidkhah, M. R., Ghobadian, B., & Ardjmand, M. (2019). Optimizing different angles of venturi in biodiesel production using cfd analysis. Iranian Journal of Chemistry and Chemical Engineering, 38(6), 285–295. https://doi.org/10.30492/ijcce.2019.32597
8. Crudo, D., Bosco, V., Cavaglià, G., Grillo, G., Mantegna, S., & Cravotto, G. (2016). Biodiesel production process intensification using a rotor-stator type generator of hydrodynamic cavitation. Ultrasonics Sonochemistry, 33, 220–225. https://doi.org/10.1016/j.ultsonch.2016.05.001
9. Demirbas, A. (2009). Biofuels from agricultural biomass. *Energy Sources, Part A, 31*(17), 1573-1582. https://doi.org/10.1080/15567030802094011
10. Dwivedi, G., Jain, S., & Sharma, M. (2011). Impact analysis of biodiesel on engine performance—A review. *Renewable and Sustainable Energy Reviews, 15*(9), 4633-4641. https://doi.org/10.1016/j.rser.2011.07.089
11. Elgharbawy, a. S., sadik, w. A., sadek, o. M., & kasaby, m. A. (2021). A review on biodiesel feedstocks and production technologies. Journal of the Chilean Chemical Society, 65(1), 5098–5109. https://doi.org/10.4067/S0717-97072021000105098
12. Feng, H., Barbosa-Cánovas, G. V., & Weiss, J. (2011). Ultrasound technologies for food and bioprocessing. https://link.springer.com/book/10.1007/978-1-4419-7472-3
13. Franke, M., Ondruschka, B., & Braeutigam, P. (2014). Hydrodynamic-Acoustic-Cavitation for Biodiesel Synthesis. Ipcbee, 78(6). Retrieved from 13. Franke, M., Ondruschka, B., & Braeutigam, P. (2014). Hydrodynamic-Acoustic-Cavitation for Biodiesel Synthesis. Ipcbee, 78(6).
14. Li, H. L., & Yu, P. H. (2015). Conversion of waste cooking oils into environmentally friendly biodiesel. *SpringerPlus*. https://doi.org/10.1186/2193-1801-4-S2-P7

15. Gharat, N., & Rathod, V. K. (2013). Enzyme catalyzed transesterification of waste cooking oil with dimethyl carbonate. *Journal of Molecular Catalysis B: Enzymatic, 88*(0), 36-40. http://dx.doi.org/10.1016/j.molcatb.2012.11.007

16. Ghobadian, B., Rahimi, H., Tavakkoli Hashjin, T., & Khatamifar, M. (2010). Production of bioethanol and sunflower methyl ester and investigation of fuel blend properties. *Journal of Agricultural Science and Technology, 10*, 225-232. http://dorl.net/dor/20.1001.1.16807073.2008.10.3.9.5

17. Gogate, P. R., & Bhosale, G. S. (2013). Comparison of effectiveness of acoustic and hydrodynamic cavitation in combined treatment schemes for degradation of dye wastewaters. *Chemical Engineering and Processing: Process Intensification, 71*, 59-69. https://doi.org/10.1016/j.cep.2013.03.001

18. Gomez-Exposito, A., Conejo, A. J., & Canizares, C. (2018). *Electric energy systems: analysis and operation*: CRC press. https://www.routledge.com/Electric-Energy-Systems-Analysis-and-Operation/Gomez-Exposito-Conejo-Canizares/p/book/9780367734275?srsltid=AfmBOoqlkaIhgKKpIWd20JChFEFBpvhRHmKzJGTpMAtGrrf25EmQpRH8

19. Ivleva, T. P., Merzhanov, A. G., Rumanov, E. N., Vaganova, N. I., Campbell, A. N., & Hayhurst, A. N. (2011). When do chemical reactions promote mixing? *Chemical Engineering Journal*, *168*(1), 1–14. https://doi.org/10.1016/j.cej.2011.01.002

20. Kayode, B., & and Hart, A. (2019). An overview of transesterification methods for producing biodiesel from waste vegetable oils. *Biofuels*, *10*(3), 419–437. https://doi.org/10.1080/17597269.2017.1306683

21. Kelkar, M. A., Gogate, P. R., & Pandit, A. B. (2008). Intensification of esterification of acids for synthesis of biodiesel using acoustic and hydrodynamic cavitation. *Ultrasonics Sonochemistry, 15*(3), 188-194. https://doi.org/10.1016/j.ultsonch.2007.04.003

22. Khan, E., Ozaltin, K., Spagnuolo, D., Bernal-Ballen, A., Piskunov, M. V, & Di Martino, A. (2023). Biodiesel from Rapeseed and Sunflower Oil: Effect of the Transesterification Conditions and Oxidation Stability. *Energies*. https://www.researchgate.net/publication/366942281

23. Liu, K., & Wang, R. (2013). Biodiesel production by transesterification of duck oil with methanol in the presence of alkali catalyst. *Petroleum & Coal, 55*(1), 68-72. https://www.researchgate.net/publication/286586863

24. Lobanoff, V. S., & Ross, R. R. (2013). *Centrifugal pumps: design and application*: Elsevier. https://shop.elsevier.com/books/centrifugal-pumps/lobanoff/978-0-08-050085-0

25. Lopresto, C. G. (2025). Sustainable biodiesel production from waste cooking oils for energetically independent small communities: an overview. *International Journal of Environmental Science and Technology*, *22*(3), 1953–1974. https://doi.org/10.1007/s13762-024-05779-2

26. Marchetti, J., Miguel, V., & Errazu, A. (2007). Possible methods for biodiesel production. *Renewable and sustainable energy reviews, 11*(6), 1300-1311. https://doi.org/10.1016/j.rser.2005.08.006

27. Mohammed, Z., & Mohand, K. (2015). Analysis of cavitating flow through a venturi. *Scientific Research and Essays*, *10*(11), 367–375. https://doi.org/10.5897/sre2015.6201

28. Monika, Banga, S., & Pathak, V. V. (2023). Biodiesel production from waste cooking oil: A comprehensive review on the application of heterogenous catalysts. *Energy Nexus*, *10*, 100209. https://doi.org/10.1016/j.nexus.2023.100209

29. Oo, Y. M., Juera-Ong, P., & Somnuk, K. (2024). Methyl ester production process from palm fatty acid distillate using hydrodynamic cavitation reactors in series with solid acid catalyst. Scientific Reports, 14(1), 27732. https://doi.org/10.1038/s41598-024-78974-3

30. Ozonek, J. K. L. (2011). Effect of different design features of the reactor on hydrodynamic cavitation process. *Archives of Materials Science and Engineering, 52*(2), 112-117. https://www.researchgate.net/publication/267709862

31. Pal, A., Mohan, S., & Trivedi, D. (2014). Production and Performance Testing of Waste Frying Oil Biodiesel. https://inpressco.com/wp-content/uploads/2014/05/Paper301366-1369.pdf

32. Pal, A., Verma, A., Kachhwaha, S., & Maji, S. (2010). Biodiesel production through hydrodynamic cavitation and performance testing. *Renewable Energy, 35*(3), 619-624. https://doi.org/10.1016/j.renene.2009.08.027

33. Patil, A., Baral, S., & Dhanke, P. (2021). Hydrodynamic cavitation for process intensification of biodiesel synthesis- a review. Current Research in Green and Sustainable Chemistry, 4(April), 100144. https://doi.org/10.1016/j.crgsc.2021.100144

34. Streeter, V. L., Wylie, E. B., & Bedford, K. W. (1998). Fluid mechanics, WCB: McGraw-Hill. https://books.google.com/books/about/Fluid_Mechanics.html?id=oJ5RAAAAMAAJ

35. Tavizón-Pozos, J. A., Chavez-Esquivel, G., Suárez-Toriello, V. A., Santolalla-Vargas, C. E., Luévano-Rivas, O. A., Valdés-Martínez, O. U., … Rodriguez, J. A. (2021). State of Art of Alkaline Earth Metal Oxides Catalysts Used in the Transesterification of Oils for Biodiesel Production. *Energies*. https://doi.org/10.3390/en14041031

36. Tullis, J. P. (1989). *Hydraulics of pipelines: pumps, valves, cavitation, transients*: John Wiley & Sons. https://onlinelibrary.wiley.com/doi/book/10.1002/9780470172803

37. Wan Osman, W. N. A., Rosli, M. H., Mazli, W. N. A., & Samsuri, S. (2024). Comparative review of biodiesel production and purification. *Carbon Capture Science & Technology*, *13*, 100264. https://doi.org/10.1016/j.ccst.2024.100264

38. Worapun, I., Pianthong, K., Applied, P. T.-E. and, & 2010, undefined. (n.d.). Synthesis of biodiesel by two-step transesterification from crude jatropha curcus L. oil using ultrasonic irradiation assisted. Thaiscience.Info. https:/www.thaiscience.info/journals/Article/KKEJ/10889860.pdf

39. Zapater, D., Kulkarni, S. R., Wery, F., Cui, M., Herguido, J., Menendez, M., … Castaño, P. (2024). Multifunctional fluidized bed reactors for process intensification. *Progress in Energy and Combustion Science*, *105*, 101176. https://doi.org/10.1016/j.pecs.2024.101176

40. Zheng, H., Zheng, Y., & Zhu, J. (2022). Recent Developments in Hydrodynamic Cavitation Reactors: Cavitation Mechanism, Reactor Design, and Applications. *Engineering*, *19*, 180–198. https://doi.org/10.1016/j.eng.2022.04.027